Brief Definitive Report

BLTR Mediates Leukotriene B_4–induced Chemotaxis and Adhesion and Plays a Dominant Role in Eosinophil Accumulation in a Murine Model of Peritonitis

By Andrew M. Tager,* Jennifer H. Dufour,* Katayoon Goodarzi,‡ Scott D. Bercury,* Ulrich H. von Andrian,‡ and Andrew D. Luster*

*From the *Center for Immunology and Inflammatory Diseases, Division of Rheumatology, Allergy and Immunology, Massachusetts General Hospital, Harvard Medical School, Boston, Massachusetts 02114; and the ‡Center for Blood Research and Department of Pathology, Harvard Medical School, Boston, Massachusetts 02115*

Abstract

Leukotriene B_4 (LTB_4) is a potent chemoattractant active on multiple leukocytes, including neutrophils, macrophages, and eosinophils, and is implicated in the pathogenesis of a variety of inflammatory processes. A seven transmembrane–spanning, G protein–coupled receptor, called BLTR (LTB_4 receptor), has recently been identified as an LTB_4 receptor. To determine if BLTR is the sole receptor mediating LTB_4-induced leukocyte activation and to determine the role of LTB_4 and BLTR in regulating leukocyte function in inflammation in vivo, we generated a BLTR-deficient mouse by targeted gene disruption. This mouse reveals that BLTR alone is responsible for LTB_4-mediated leukocyte calcium flux, chemotaxis, and firm adhesion to endothelium in vivo. Furthermore, despite the apparent functional redundancy with other chemoattractant–receptor pairs in vitro, LTB_4 and BLTR play an important role in the recruitment and/or retention of leukocytes, particularly eosinophils, to the inflamed peritoneum in vivo. These studies demonstrate that BLTR is the key receptor that mediates LTB_4-induced leukocyte activation and establishes a model to decipher the functional roles of BLTR and LTB_4 in vivo.

Key words: receptors • leukotriene • chemotactic factors • inflammation mediators • knockout

Introduction

Leukotrienes are potent biological mediators of inflammation generated from arachidonic acid via the 5-lipoxygenase pathway (1, 2). Leukotriene B_4 (LTB_4) primarily mediates leukocyte recruitment and activation. LTB_4 was discovered based on its potent chemotactic activity on neutrophils (3) but is also active on eosinophils (4, 5). LTB_4-mediated leukocyte recruitment is thought to play a protective role in host defense against various pathogens. However, LTB_4 is also involved in the pathogenesis of a wide variety of human inflammatory diseases (1, 2), and LTB_4 receptor(s) therefore represent attractive targets for therapeutic intervention.

Although chemoattractants constitute a diverse array of molecules, including lipids, proteins, and peptides, they all appear to signal leukocytes through a subgroup of the G protein–coupled, seven transmembrane–spanning family of receptors. Members of this group of receptors are related in structure and function and include a receptor for LTB_4 (BLTR) (6, 7). We previously reported the molecular cloning of murine (m)BLTR while searching for novel chemoattractant receptors expressed in murine eosinophils and demonstrated that it encodes a functional receptor for LTB_4 (5).

BLTR function in leukocyte chemoattraction has been demonstrated in vivo by the ability of synthetic BLTR antagonists to reduce leukocyte recruitment in murine models of inflammatory diseases (8–10). However, studies of pharmacologic antagonists may be limited by several factors, including partial preservation of receptor activity in the face of the antagonist, difficulty with maintaining an inhibitory concentration of the antagonist, and unanticipated secondary effects of the antagonist administered. Studies of BLTR antagonists may also be limited by lack of specificity of these agents for BLTR, as they may modulate other receptors, including other receptors for LTB_4. For example, LTB_4 has been demonstrated to be a natural ligand for the nuclear receptor peroxisome proliferator-activated receptor

Address correspondence to Andrew D. Luster, Massachusetts General Hospital, Bldg. 149, 13th St., Charlestown, MA 02129. Phone: 617-726-5710; Fax: 617-726-5411; E-mail: luster@helix.mgh.harvard.edu

(PPAR)α (11). Whereas BLTR appears to mediate the proinflammatory leukocyte recruitment induced by LTB$_4$, PPARα activation appears to have antiinflammatory effects, as suggested by the observation of prolonged inflammation in PPARα-deficient mice when challenged with LTB$_4$ or its precursor, arachidonic acid (11).

To determine whether BLTR is the sole receptor mediating LTB$_4$-induced leukocyte recruitment and activation and whether LTB$_4$ and BLTR play unique roles in inflammation in vivo, we generated a BLTR-deficient (BLTR$^{-/-}$) mouse by targeted gene disruption. Analysis of this mouse reveals that BLTR alone is responsible for multiple functions involved in LTB$_4$-mediated leukocyte recruitment: calcium flux, chemotaxis, and firm adhesion to endothelium in vivo. Furthermore, despite functional redundancy with other chemoattractant–receptor pairs in vitro, LTB$_4$ and BLTR play important roles in the recruitment and/or retention of leukocytes, particularly eosinophils, in a murine model of peritonitis.

Materials and Methods

Targeted Disruption of the BLTR Gene. An $\sim$16-kb genomic DNA fragment containing mBLTR was isolated from a 129/SvJ genomic phage library (Stratagene) using the mBLTR cDNA (5) as a probe. The BLTR genomic locus was modified by inserting a neomycin resistance cassette into the open reading frame contained in exon 2, near the proposed initiating methionine. This construct was introduced into J1 embryonic stem (ES) cells by electroporation, and transfected cells were selected for neomycin resistance by addition of the antibiotic G418. Two clones that showed evidence of homologous recombination by Southern blotting were injected into blastocysts using standard techniques. After reimplantation into foster mothers, these clones resulted in chimeric mice that transmitted the disrupted allele to offspring. Mice were genotyped by Southern blot and PCR analysis of DNA extracts from tail snips using standard techniques. In all experiments, BLTR-deficient and control wild-type mice were generated from matings between heterozygous (BLTR$^{+/-}$) mice of similar genetic backgrounds (129/SvJ and C57BL/6 hybrids) and raised in identical specific pathogen–free conditions.

Purification of Mouse Leukocytes. Blood for hematocrits, white blood cell counts, and differentials was obtained by cardiac puncture. Peritoneal cells were harvested by peritoneal lavage with 10 ml of cold PBS without Ca^{2+} or Mg^{2+} (CMF PBS). Intraperitoneal injections of 1 ml of 3% (wt/vol) thioglycollate broth were used to elicit inflammatory cells into the peritoneal cavity. Neutrophils were harvested 4 h after thioglycollate injection and macrophages at 96 h. The cellular compositions of lavages were determined by Diff-Quik–stained (Baxter Scientific) cytocentrifuge preparations. Lavages performed 4 h after thioglycollate contained $\sim$50% neutrophils, whereas lavages performed at 96 h contained $\sim$80% macrophages. Bone marrow cells were harvested by flushing femurs with 5 ml of cold CMF PBS. Bone marrow neutrophils and mononuclear cells were purified with Neutrophil Isolation Media-2 (Cardinal Associates).

Northern Blot Analysis. RNA was isolated from mouse cells and organs, and Northern analysis was performed as described (5) using a [^{32}P]dCTP Klenow-labeled, random-primed mBLTR cDNA probe and murine glyceraldehyde-3-phosphate dehydrogenase (GAPDH) as a control of RNA loading.

Calcium Flux. Calcium fluxes in elicited peritoneal neutro-

phils and macrophages in response to the agonists LTB$_4$ and platelet-activating factor (PAF; Calbiochem) and the murine chemokines JE, KC, macrophage inflammatory protein (MIP)-1α, and eotaxin (PeproTech) were determined as described (5). The data are presented as the relative ratio of fluorescence at 340/380 nm.

Chemotaxis. 50 μl of purified mouse bone marrow neutrophils at 5.0×10^6 cells/ml in HBSS were placed in the top of a 48-well modified Boyden microchemotaxis chamber (NeuroProbe). 30 μl of 10-fold serial dilutions of LTB$_4$, KC, and FMLP (formyl-methionine-leucine-phenylalanine; Sigma-Aldrich) in HBSS were placed in the bottom wells of the chamber and were separated from the cells by a 3-μm-pore, polyvinylpyrrolidone-free polycarbonate filter. The apparatus was incubated at 37°C and 5% CO$_2$ for 60 min, and cells that migrated across the filter and adhered to the bottom side of the filter were stained with Diff-Quik and counted.

Analysis of Leukocyte Behavior by Intravital Microscopy. Mice were anesthetized by intraperitoneal injection of 200 μl of saline containing 15 mg/ml ketamine HCl (Ketaset) and 3 mg/ml xylazine (Phoenix Pharmaceuticals). The right jugular vein was catheterized with polyethylene tubing, and animals were placed on a Plexiglas stage and the right cremaster muscle (CM) was surgically prepared and superfused with sterile Ringer's injection solution as described (12). Preparations were transferred to an intravital microscope (Mikron Instruments), and 10 ml/kg saline containing 0.2% rhodamine 6G (Molecular Probes) was injected intravenously to fluorescently label circulating leukocytes, which were visualized using a 40× water immersion objective (ZEISS) and video-triggered stroboscopic epi-illumination as described (12). 1-min recordings of fluorescent cells in venular trees consisting of two to eight branches (diameter 25 ± 8 μm in BLTR$^{+/+}$ and 28 ± 8 μm in BLTR$^{-/-}$ mice) were made during up to three consecutive 5-min intervals (control period). Thereafter, the superfusion buffer was replaced with Ringer's injection solution containing 100 nM LTB$_4$. During continuous exposure to LTB$_4$, video recordings of the same venular tree were made every 5 min for 25 min. Subsequently, the fluorescent plasma marker FITC–dextran, 150 kD (Sigma-Aldrich) was injected intravenously (2 mg per mouse), and the same venular tree was recorded for measurement of vascular length and luminal diameter.

Video tapes were analyzed to compare leukocyte behavior at baseline, i.e., after mild surgical trauma, and during LTB$_4$ superfusion. The total leukocyte flux was determined by counting every fluorescent cell (rolling plus noninteracting) that passed each venule per minute. The rolling fraction was calculated by dividing the flux of rolling cells by the total leukocyte flux. The number of firmly adherent leukocytes (i.e., cells that remained stationary for at least 30 s) in the entire venular tree was determined for each time point. The luminal surface area of venular trees was calculated by measuring dimensions of FITC–dextran-filled venules, assuming cylindrical vascular geometry. The number of adherent leukocytes was divided by the luminal surface area.

FACS® Analysis. Cell suspensions in PBS containing 1% BSA were preincubated with Fc block (anti-mCD16/32; PharMingen) or 10% normal mouse serum for 15 min at 4°C before staining with primary antibodies, including anti-mCCR3 (R&D Systems). After washing, secondary antibody (FITC–anti-rat IgG2a; PharMingen) was added to cells labeled with unconjugated primary antibodies for 20 min at 4°C. Cells were then washed, fixed with 2% paraformaldehyde, and analyzed on a Becton Dickinson FACScan™ using CELLQuest™ software (Becton Dickinson).

Statistical Analysis. Differences in rolling fractions were ana-

lyzed by paired Student's *t* test, and differences in peritoneal lavage cell compositions were analyzed by analysis of variance using Statview® statistical software (Abacus Concepts, Inc.)

Results and Discussion

Targeted Disruption of the BLTR Gene. To disrupt the BLTR gene, a neomycin resistance cassette was inserted into the open reading frame in exon 2 of BLTR, just 3′ of the proposed initiating methionine (Fig. 1 A). The frequency of homologous recombination in ES cells was ~8.3% (15 of 181 G418-resistant clones). Two ES clones containing the disrupted allele were injected into blastocysts and resulted in live births after transfer to foster mothers. The chimeras from these clones passed the disrupted allele to their progeny, which were intercrossed to produce
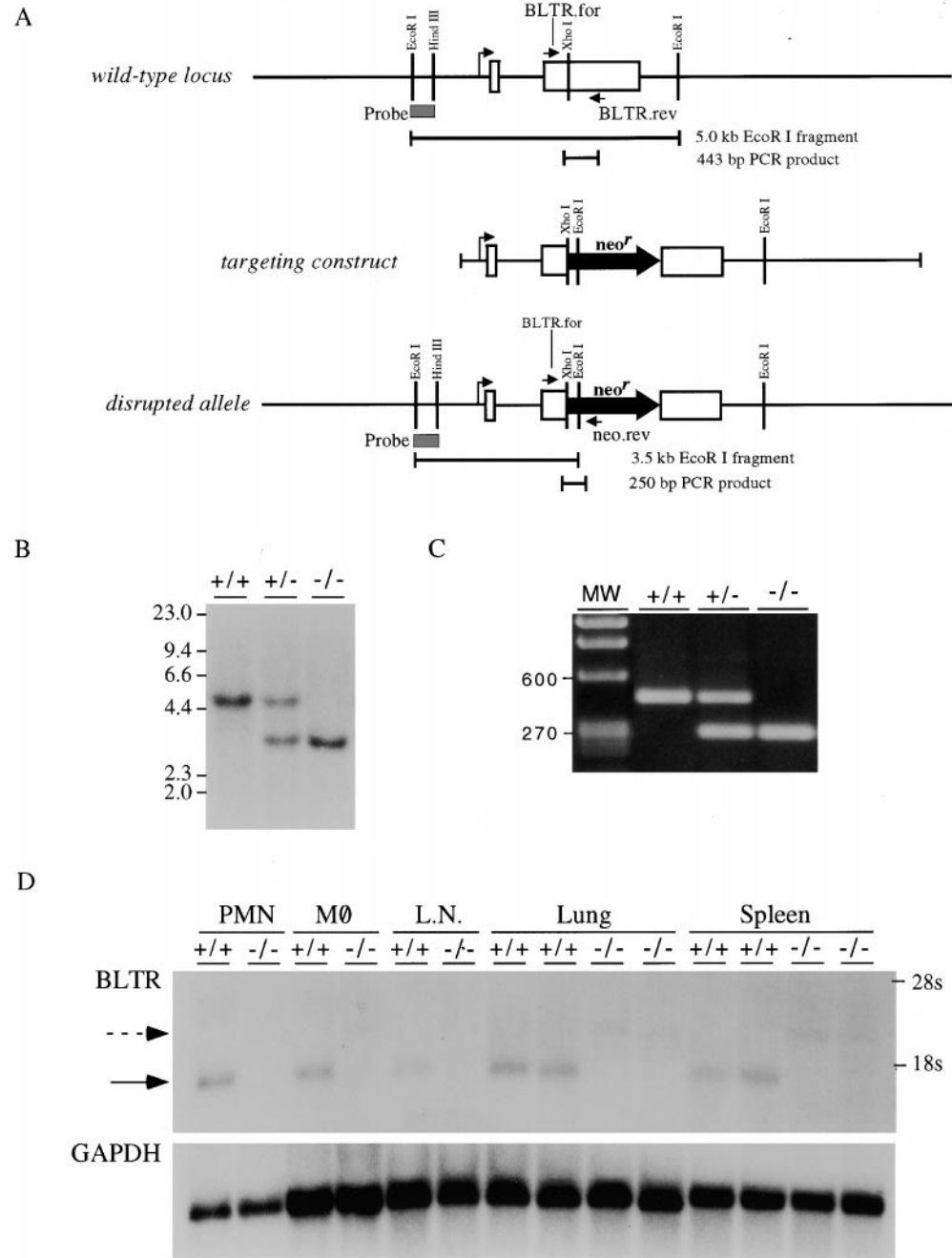
Figure 1. Generation of BLTR$^{-/-}$ mice. (A) Schematic of wild-type locus, targeting construct, and disrupted allele. The two exons encoding BLTR in the wild-type locus are shown as open boxes. The EcoRI–HindIII fragment used as a probe in Southern blotting is indicated as a shaded box. This probe identifies a 5-kb fragment of the wild-type allele upon digestion with EcoRI. PCR using the primers BLTR.for and BLTR.rev, located as shown, generates a 443-bp PCR product. The targeting construct was made by inserting the 1.85-kb neomycin resistance cassette into the XhoI site in exon 2, resulting in 2.4 kb of genomic DNA 5′ to the neomycin resistance cassette and 13.6 kb 3′ to the cassette. The EcoRI–HindIII probe identifies a 3.5-kb fragment of the disrupted allele upon digestion with EcoRI. PCR using the primers BLTR.for and neo.rev, located as shown, generates a 250-bp PCR product from the disrupted allele. (B) Southern blot analysis. DNA from wild-type mice (+/+) and mice heterozygous (+/−) or homozygous (−/−) for the disrupted BLTR allele was digested with EcoRI and analyzed by Southern blotting using the probe indicated in A. Molecular weights (MW) in kilobases are displayed on the left of the blot. (C) Genomic PCR analysis. DNA from wild-type mice (+/+) and mice heterozygous (+/−) or homozygous (−/−) for the disrupted BLTR allele was analyzed by PCR using the primers indicated in A. Molecular weights (MW) in basepairs are displayed on the left of the gel. (D) Northern blot analysis. 5 μg of RNA from neutrophils (PMN), 10 μg from macrophages (MØ), and 20 μg from lymph nodes (L.N.), lungs, and spleens of wild-type and BLTR$^{-/-}$ mice were analyzed by Northern blotting using BLTR cDNA as a probe. The locations of 28S and 18S ribosomal RNA are displayed on the right of the blot. The previously described 1.45-kb BLTR transcript (solid arrow) was identified in wild-type mice but was absent in BLTR$^{-/-}$ mice, being replaced by a larger transcript (dashed arrow). This larger transcript, which resulted from the insertion of the neomycin resistance cassette in exon 2 of the BLTR gene, was detected at lower levels than the wild-type transcript, which is often seen for hybrid transcripts generated from gene-targeted alleles.

mice homozygous for the disrupted allele. Mice were genotyped by Southern blot analysis of DNA digested with EcoRI (Fig. 1 B) and confirmed by PCR analysis (Fig. 1 C). The disrupted allele was passed through the germline with a Mendelian inheritance pattern. Homozygous $BLTR^{-/-}$ mice were viable, fertile, and without any gross developmental defects.

To confirm that BLTR expression had been disrupted, Northern blot analysis was performed with RNA isolated from neutrophils, macrophages, lymph nodes, lungs, and spleens of wild-type and homozygous $BLTR^{-/-}$ mice (Fig. 1 D). This analysis revealed the previously described 1.45-kb BLTR transcript in wild-type mice. Homozygous gene-targeted mice did not have this 1.45-kb BLTR transcript but instead had a larger BLTR mRNA transcript due to the insertion of the neomycin resistance cassette in exon 2 of the BLTR gene.

BLTR Mediates LTB$_4$-induced Calcium Flux in Neutrophils and Macrophages. Signaling through G protein–coupled, seven transmembrane–spanning chemoattractant receptors typically generates a transient rise in intracellular calcium. We investigated the ability of LTB$_4$ to induce a calcium flux in thioglycollate-elicited peritoneal neutrophils and macrophages. LTB$_4$ induced rapid calcium fluxes in both cell types from wild-type mice but not in either cell type isolated from $BLTR^{-/-}$ mice (Fig. 2). In separate experiments, LTB$_4$ at a higher concentration (333 nM) also failed to induce calcium fluxes in neutrophils from $BLTR^{-/-}$ mice (data not shown). Additionally, LTB$_4$ induced desensitization in wild-type neutrophils and macrophages, demonstrating normal signaling in these leukocyte preparations. Calcium flux responses to chemokines KC and MIP-1α

and the lipid chemoattractant PAF were preserved in neutrophils from $BLTR^{-/-}$ mice and were comparable to those induced in wild-type neutrophils. Similarly, calcium fluxes in response to the chemokines JE (murine monocyte chemoattractant protein 1) and MIP-1α as well as PAF in macrophages from $BLTR^{-/-}$ mice were comparable to those induced in wild-type macrophages. Although the response of $BLTR^{-/-}$ macrophages shown in Fig. 2 demonstrates a minimal calcium flux in response to MIP-1α, this chemokine produced robust fluxes in these cells in other experiments (data not shown). These results demonstrate that BLTR specifically mediates LTB$_4$-induced calcium flux responses in both neutrophils and macrophages. The responses of the neutrophil preparations to the neutrophil-specific chemokine KC but not to the monocyte/macrophage-specific chemokine JE confirmed the presence of responsive neutrophils in those preparations. Likewise, the responses of the macrophage preparations to the monocyte/macrophage-specific chemokine JE but not the neutrophil-specific chemokine KC confirmed the presence of responsive macrophages but not neutrophils in those preparations.

BLTR Mediates LTB$_4$-induced Chemotaxis. As LTB$_4$ is known to be a potent neutrophil chemoattractant, we investigated the ability of LTB$_4$ to induce chemotaxis in neutrophils isolated from the bone marrow of wild-type and $BLTR^{-/-}$ mice. While LTB$_4$ induced a typical dose-dependent chemotaxis of wild-type neutrophils (peak chemotaxis at 100 nM), it had no effect on neutrophils isolated from $BLTR^{-/-}$ mice (Fig. 3). As positive controls, both FMLP and KC induced comparable chemotaxis of neutrophils isolated from wild-type and $BLTR^{-/-}$ mice.
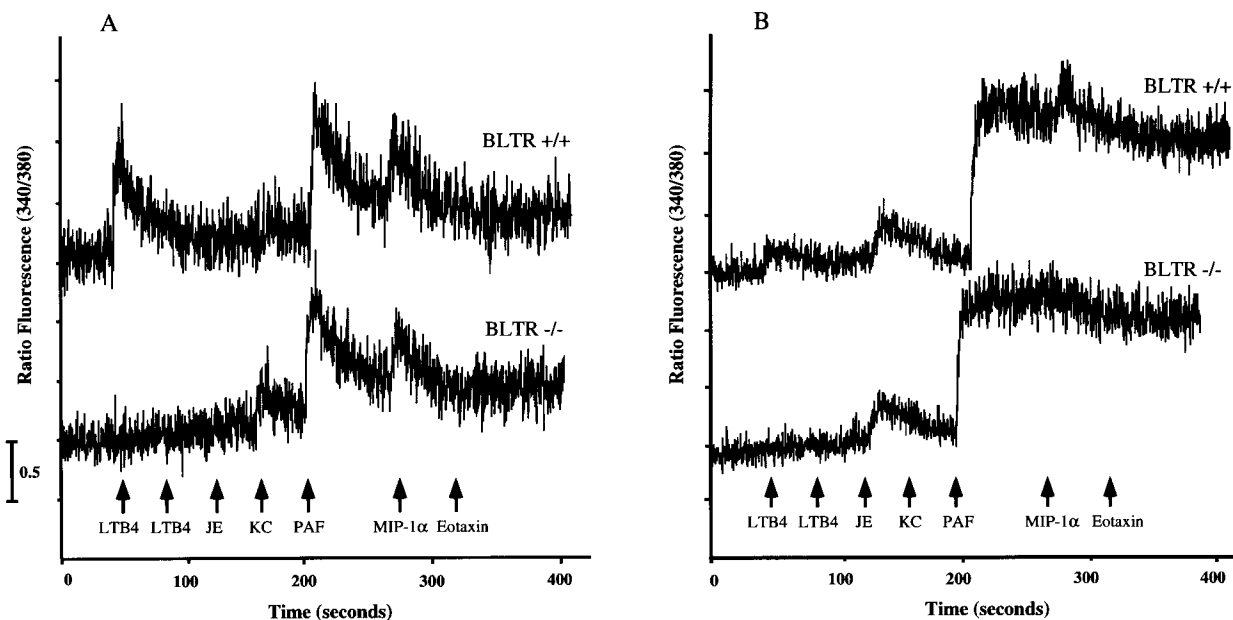
Figure 2. Calcium flux responses of wild-type and $BLTR^{-/-}$ leukocytes. Each tracing represents the intracellular $[Ca^{2+}]$ levels of fura-2–loaded peritoneal neutrophils (A) or macrophages (B) measured as relative fluorescence over time. Arrows mark the time of addition of the indicated agonists at optimal concentrations: LTB$_4$ (167 nM), JE (20 nM), KC (20 nM), PAF (167 nM), MIP-1α (20 nM), and eotaxin (20 nM). The results shown are representative experiments ($n = 3$–4 for all cell types).
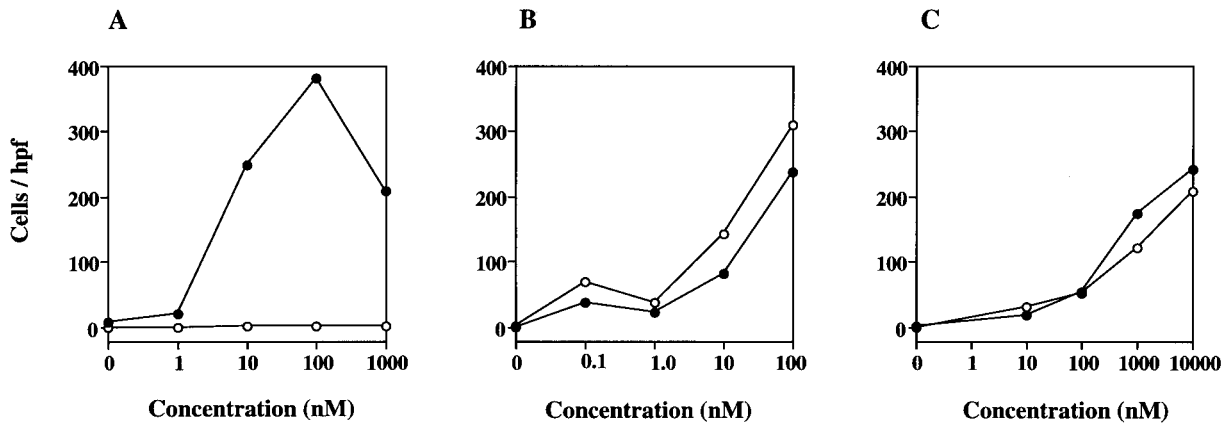
Figure 3. Chemotactic responses of wild-type (●) and BLTR$^{-/-}$ (○) bone marrow neutrophils to LTB$_4$ (A), KC (B), and FMLP (C). Neutrophils were exposed to increasing concentrations of the indicated chemoattractants in a modified Boyden chamber, and the numbers of cells that migrated through the membrane were determined. Data are the number of cells per 400× field (hpf). The results shown are representative experiments ($n = 3$) and presented as the mean of eight fields counted from replicate wells.

These results demonstrate that BLTR specifically mediates LTB$_4$-induced neutrophil chemotaxis.

BLTR Mediates LTB$_4$-induced Leukocyte Arrest in CM Venules. Firm adhesion within blood vessels is a prerequisite for leukocyte migration into tissues. In most settings, rolling leukocytes must encounter a chemotactic stimulus that triggers rapid activation of integrins, which mediate firm arrest. Previous intravital microscopy studies have shown that topically applied LTB$_4$ is a potent inducer of integrin-mediated arrest of murine leukocytes (12). The data shown above demonstrate that BLTR is essential for leukocyte chemotaxis. However, chemotaxis is a slow process lasting minutes to hours, whereas integrin-mediated arrest occurs within seconds or less. Recent studies suggest that chemoattractant-induced chemotaxis and arrest are distinct leukocyte functions, suggesting that they are mediated by divergent signaling pathways (13). Thus, it remained to be determined whether BLTR is as essential for rapid integrin activation as it is for chemotaxis. We performed intravital microscopy to investigate the effect of BLTR deficiency on LTB$_4$-induced leukocyte arrest in CM venules of wild-type and BLTR$^{-/-}$ mice. As shown previously (12), LTB$_4$ induced a marked accumulation of adherent leukocytes in wild-type mice in a time-dependent fashion. In contrast, there was no change in the number of adherent cells above spontaneous background adhesion in BLTR$^{-/-}$ mice (Fig. 4).

It has been well established that chemoattractant-mediated leukocyte arrest must be preceded by selectin-dependent leukocyte rolling (14). To investigate whether BLTR deficiency affects rolling, we determined rolling fractions in CM venules. There was no significant difference when wild-type and BLTR$^{-/-}$ mice were compared during the control period (36 ± 11% and 41 ± 21%, respectively [mean ± SD]). LTB$_4$ superfusion did not alter rolling in BLTR$^{-/-}$ mice (35 ± 15% at 20 min of continuous superfusion), but rolling decreased significantly in wild-type mice (9 ± 12% at 20 min; $P < 0.05$). This decrease in roll-

ing fraction in the presence of a chemotactic stimulus has been observed previously (14). In all, these data are consistent with a normal response to LTB$_4$ in wild-type mice and a complete lack of responsiveness in the BLTR$^{-/-}$ animals. We conclude that BLTR is not involved in trauma-induced leukocyte rolling mediated by selectins but that it is essential for LTB$_4$-induced, rapid, integrin-mediated arrest of the rolling cells.
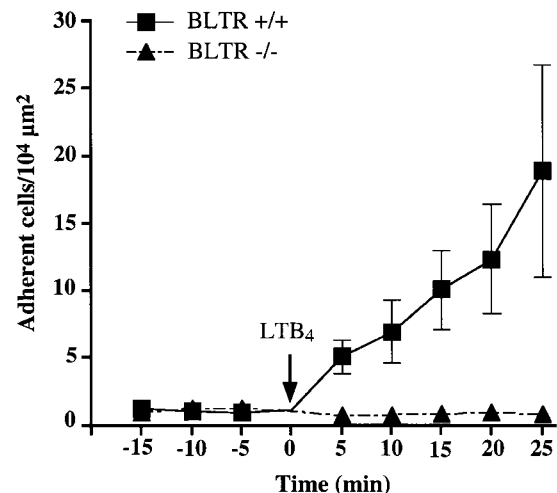

Figure 4. Firm adhesion of wild-type and BLTR$^{-/-}$ leukocytes determined by intravital microscopy. Fluorescently labeled leukocytes in a representative venular tree (consisting of two to eight venular branches) were videotaped under epifluorescence illumination. Symbols represent the mean adherent leukocyte density as described in Materials and Methods. During a 15-min control period, CM preparations were superfused with sterile bicarbonate–buffered Ringer's injection solution, and baseline leukocyte adherence was assessed at least once. In some animals, baseline adherence was analyzed three times in 5-min intervals; no spontaneous changes in baseline rolling or adherence were observed (data not shown). At time point 0 min, the superfusion buffer was rapidly exchanged for Ringer's injection solution containing 100 nM LTB$_4$, and leukocyte adherence was quantitated in the same venular tree at the indicated time points ($n = 20$ venules in four BLTR$^{+/+}$ mice; $n = 19$ venules in three BLTR$^{-/-}$ mice)

BLTR Mediates Leukocyte Recruitment in Thioglycollate-induced Peritonitis. Intraperitoneal instillation of thioglycollate in wild-type mice induces an inflammatory response that includes the recruitment of neutrophils, eosinophils, and macrophages. Leukocyte recruitment in this model has been shown to be at least partially leukotriene dependent in that recruitment is diminished by inhibition of 5-lipoxygenase (15). We therefore quantified the contribution of BLTR and LTB_4 to the in vivo recruitment of neutrophils and eosinophils, for

which LTB_4 has potent chemotactic activity, as well as macrophages, which we have previously demonstrated to express BLTR (5), in this model. Compared with untreated animals, total peritoneal leukocytes increased 4 h after thioglycollate instillation, peaked at 48 h, and then declined slightly by 96 h in both $BLTR^{-/-}$ and wild-type mice (Fig. 5 A). At 96 h, $BLTR^{-/-}$ mice had only 61% as many leukocytes recovered from the peritoneal cavity as wild-type mice ($P < 0.05$).

Of the three types of leukocytes recruited, neutrophils,

A
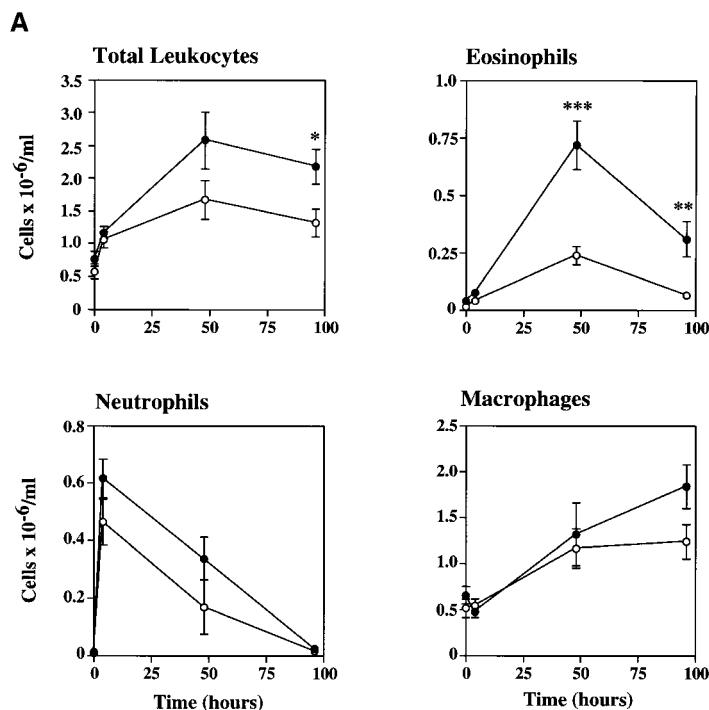
Figure 5. Leukocyte recruitment in thioglycollate-induced peritonitis in wild-type (●) and $BLTR^{-/-}$ (○) mice. (A) Total numbers of leukocytes, eosinophils, neutrophils, and macrophages are presented as the mean number of these cells (±SE) obtained by peritoneal lavage at baseline and 4, 48, and 96 h after intraperitoneal injection of thioglycollate in 5–10 mice of each genotype. Cell type was determined by morphological analyses of Diff-Quik–stained cytocentrifuge preparations by an observer blinded to genotype. *$P < 0.05$; **$P < 0.01$; ***$P < 0.005$. (B) Percentages of peritoneal cells attributable to recruited eosinophils were confirmed by flow cytometric analysis at 48 and 96 h after thioglycollate injection. 25,000 events were analyzed for forward and side light scatter properties and for expression of mCCR3. Values represent the percentage of the total cell population that falls into the indicated region (R1). The broken line histogram indicates the isotype control; whereas the bold line histogram shows mCCR3 staining of the gated population (R1). These results are representative of four or five 6–10-wk-old mice of each genotype.

B
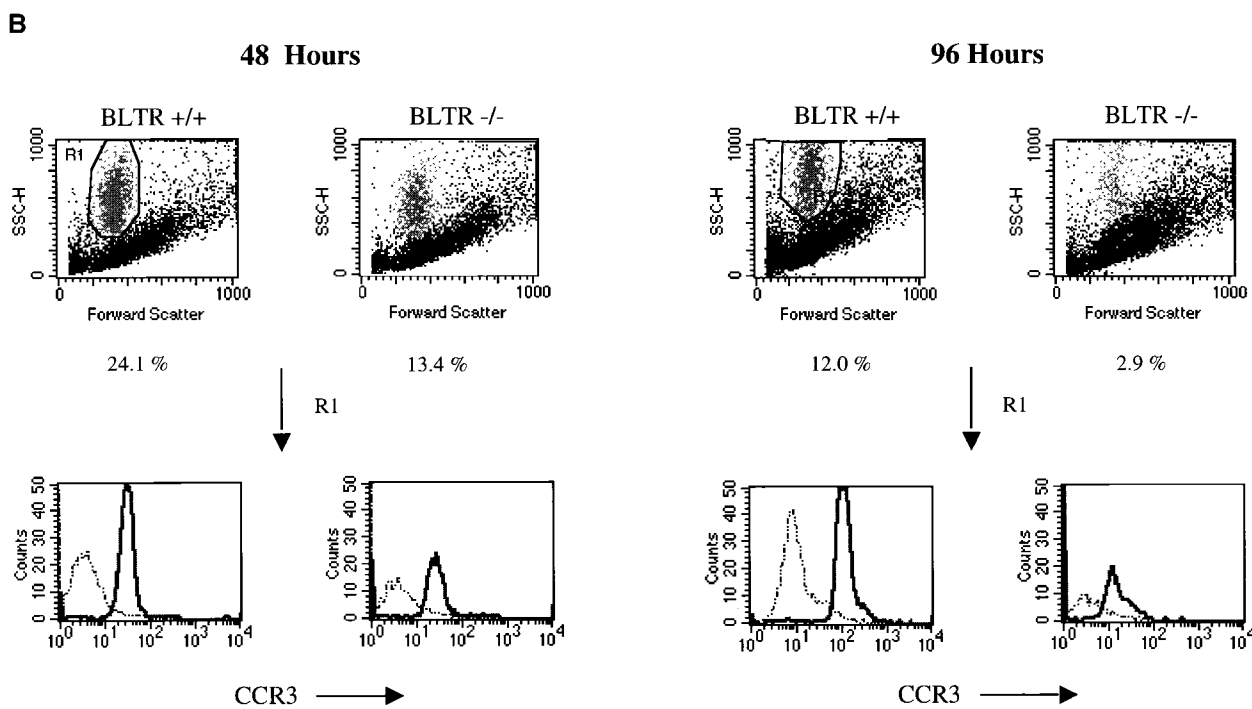
eosinophils, and macrophages, the most striking difference between BLTR$^{-/-}$ and wild-type mice occurred in eosinophil recruitment (Fig. 5 A). Neither group had substantial numbers of peritoneal eosinophils at baseline or 4 h after thioglycollate instillation. Peak numbers of eosinophils were seen in both groups at 48 h, but BLTR$^{-/-}$ mice recruited only 33% as many eosinophils to the inflamed peritoneum as wild-type mice at this time point ($P < 0.005$). Numbers of peritoneal eosinophils declined in both groups at 96 h, but BLTR$^{-/-}$ mice continued to have significantly fewer of these cells. At 96 h, BLTR$^{-/-}$ mice had only 20% as many eosinophils recovered from the peritoneal cavity as wild-type mice ($P < 0.01$).

Although the numbers of peritoneal neutrophils and macrophages appeared lower in the BLTR$^{-/-}$ mice at some time points, the differences from wild type did not reach statistical significance for either of these cell types (Fig. 5 A).

The marked reduction of eosinophil recruitment to the inflamed peritoneum after thioglycollate instillation was confirmed by flow cytometric analysis of leukocytes recovered in peritoneal lavages (Fig. 5 B). CCR3 is the receptor for the eosinophil-specific chemokine eotaxin, and eosinophils were identified by their positive reactivity with anti-mCCR3 (16) and F4/80 (17) antibodies, their negative staining with Ly6G (Gr-1) antibody (18), and by their forward and side scatter properties characteristic of granulocytes (gate R1; Fig. 5 B). These flow cytometry markers used to positively identify eosinophils were validated using spleen cells from IL-5–transgenic mice (data not shown), which are composed of 30–50% eosinophils (19). 48 h after thioglycollate instillation, eosinophils represented 24.1% of peritoneal cells recovered from wild-type mice but only 13.4% of cells from BLTR$^{-/-}$ mice as determined by flow cytometry (Fig. 5 B). In comparison, eosinophils identified by morphological analysis of Diff-Quik–stained cytocentrifuge preparations at this time point accounted for 27.8% of wild-type peritoneal cells but only 14.2% of BLTR$^{-/-}$ cells. 96 h after thioglycollate, eosinophils as identified by flow cytometry represented 12.0% of peritoneal cells recovered from wild-type mice but only 2.9% of cells from BLTR$^{-/-}$ mice. As determined by morphological analyses of Diff-Quik–stained cytocentrifuge preparations, eosinophils represented 14.2% of wild-type peritoneal cells at this time point but only 4.6% of BLTR$^{-/-}$ cells. Thus, at both 48 and 96 h after intraperitoneal injection of thioglycollate, there were significantly fewer eosinophils recruited to the inflamed peritoneum in BLTR$^{-/-}$ mice compared with wild-type mice, as determined by two different methods, morphologic analyses of cytospins and flow cytometry, which gave similar results. Flow cytometry also demonstrated no difference in the numbers of B cells, T cells, or NK cells in the peritoneum at 48 or 96 h after thioglycollate instillation, as demonstrated by comparable staining with antibodies to B220, CD3, CD4, CD8, and NK1.1 (data not shown).

Flow cytometric analysis of bone marrow using the same panel of antibodies as for the peritoneal cells and morphologic analysis of Wright-Giemsa–stained blood smears revealed no differences in leukocyte composition in untreated BLTR$^{-/-}$ and wild-type mice in either bone marrow or blood compartments (data not shown). Additionally, neither genotype had substantial numbers of eosinophils in the peritoneal cavity at baseline. Therefore, the decreased numbers of eosinophils recovered from BLTR$^{-/-}$ mice 48 and 96 h after thioglycollate appear attributable to decreased eosinophil recruitment and/or retention in this model. The delayed appearance of eosinophils is consistent with their being recruited by chemoattractants, such as LTB$_4$, produced by leukocytes preceding the eosinophils into the peritoneal cavity. The threefold reduction in recruited eosinophils seen in the BLTR$^{-/-}$ mice at 48 h and the fivefold reduction seen at 96 h indicates that LTB$_4$ and BLTR play a dominant role in eosinophil accumulation in the peritoneum after thioglycollate instillation.

In summary, we have demonstrated that BLTR alone is responsible for mediating three distinct leukocyte functions induced by LTB$_4$: calcium flux, chemotaxis, and firm adhesion under flow in vivo. Additionally, in spite of the activity of multiple chemoattractants upon eosinophils in vitro, our data demonstrate that loss of BLTR alone is sufficient to substantially diminish eosinophil recruitment in a murine model of peritonitis. Studies of other inflammatory models in the BLTR$^{-/-}$ mice will give insight into the roles of LTB$_4$ in human diseases.

References

1. Samuelsson, B., S.E. Dahlen, J.A. Lindgren, C.A. Rouzer, and C.N. Serhan. 1987. Leukotrienes and lipoxins: structures, biosynthesis, and biological effects. *Science.* 237:1171–1176.
2. Lewis, R.A., K.F. Austen, and R.J. Soberman. 1990. Leukotrienes and other products of the 5-lipoxygenase pathway. Biochemistry and relation to pathobiology in human diseases. *N. Engl. J. Med.* 323:645–655.
3. Ford-Hutchinson, A.W., M.A. Bray, M.V. Doig, M.E. Shipley, and M. Smith. 1980. Leukotriene B$_4$, a potent chemokinetic and aggregating substance released from polymorphonuclear leukocytes. *Nature.* 286:264–265.
4. Ng, C.F., F.F. Sun, B.M. Taylor, M.S. Wolin, and P.Y.-K. Wong. 1991. Functional properties of guinea pig eosinophil leukotriene B$_4$ receptor. *J. Immunol.* 147:3096–3103.
5. Huang, W.W., E.A. Garcia-Zepeda, A. Sauty, H. Oettgen, M.E. Rothenberg, and A.D. Luster. 1998. Molecular and biological characterization of the murine leukotriene B$_4$ receptor expressed on eosinophils. *J. Exp. Med.* 188:1063–1074.

6. Murphy, P.M. 1994. The molecular biology of leukocyte chemoattractant receptors. *Annu. Rev. Immunol.* 12:593–633.
7. Yokomizo, T., T. Izumi, K. Chang, Y. Takuwa, and T. Shimizu. 1997. A G-protein-coupled receptor for leukotriene B_4 that mediates chemotaxis. *Nature.* 387:620–624.
8. Fretland, D.J., C.P. Anglin, D. Widomski, D.A. Baron, T. Maziasz, and P.F. Smith. 1995. Pharmacological activity of the second generation leukotriene B_4 receptor antagonist, SC-53228: effects on acute colonic inflammation and hepatic function in rodents. *Inflammation.* 19:503–515.
9. Gladue, R., L. Carroll, A. Milici, D. Scampoli, H. Stukenbrok, E. Pettipher, E. Salter, S. Contillo, and H. Showell. 1996. Inhibition of leukotriene B_4-receptor interaction suppresses eosinophil infiltration and disease pathology in a murine model of experimental allergic encephalomyelitis. *J. Exp. Med.* 183:1893–1898.
10. Showell, H.J., M.J. Conklyn, R. Alpert, G.P. Hingorani, K.F. Wright, M.A. Smith, E. Stam, E.D. Salter, D.N. Scampoli, S. Meltzer, et al. 1998. The preclinical pharmacological profile of the potent and selective leukotriene B_4 antagonist CP-195543. *J. Pharmacol. Exp. Ther.* 285:946–954.
11. Devchand, P., H. Keller, J. Peters, M. Vazquez, F. Gonzalez, and W. Wahli. 1996. The PPARα-leukotriene B_4 pathway to inflammation control. *Nature.* 384:39–43.
12. Coxon, A., P. Rieu, F.J. Barkalow, S. Askari, A.H. Sharpe, U.H. von Andrian, M.A. Arnaout, and T.N. Mayadas. 1996. A novel role for the beta 2 integrin CD11b/CD18 in neutrophil apoptosis: a homeostatic mechanism in inflammation. *Immunity.* 5:653–666.
13. Gerszten, R., E. Garcia-Zepeda, Y. Lim, M. Yoshida, H. Ding, M. Gimbrone, A. Luster, F. Luscinskas, and A. Rosenzweig. 1999. MCP-1 and IL-8 trigger firm adhesion of monocytes to vascular endothelium under flow conditions. *Nature.* 398:718–723.
14. Ley, K., G.J. Tangelder, and U.H. von Andrian. 1995. Modulation of leukocyte rolling in vivo. *In* Physiology and Pathophysiology of Leukocyte Adhesion. D.N. Granger and Schmid-Schonbein, editors. Oxford University Press, Oxford, UK. 217–240.
15. Lawson, C.F., H.W. Smith, and F.A. Fitzpatrick. 1986. Effect of Piriprost, a 5-lipoxygenase inhibitor, on leukocyte accumulation during thioglycollate-induced acute inflammation. *Wien. Klin. Wochenschr.* 98:110–113.
16. Grimaldi, J.C., N.X. Yu, G. Grunig, B.W. Seymour, F. Cottrez, D.S. Robinson, N. Hosken, W.G. Ferlin, X. Wu, H. Soto, et al. 1999. Depletion of eosinophils in mice through the use of antibodies specific for C-C chemokine receptor 3 (CCR3). *J. Leukoc. Biol.* 65:846–853.
17. McGarry, M.P., and C.C. Stewart. 1991. Murine eosinophil granulocytes bind the murine macrophage-monocyte specific monoclonal antibody F4/80. *J. Leukoc. Biol.* 50:471–478.
18. Lagasse, E., and I.L. Weissman. 1996. Flow cytometric identification of murine neutrophils and monocytes. *J. Immunol. Methods.* 197:139–150.
19. Dent, L.A., M. Strath, A.L. Mellor, and C.J. Sanderson. 1990. Eosinophilia in transgenic mice expressing interleukin 5. *J. Exp. Med.* 172:1425–1431.